PHOSPHOR HANDBOOK
PROCESS, PROPERTIES, AND APPLICATIONS

Edited by
VIJAY B. PAWADE
RITESH L. KOHALE
SANJAY J. DHOBLE
HENDRIK C. SWART

ELSEVIER

Woodhead Publishing Series in Electronic and Optical Materials

Phosphor Handbook

Process, Properties, and Applications

Edited by

Vijay B. Pawade

Department of Applied-Physics, Laxminarayan Institute of Technology, Rashtrasant Tukadoji Maharaj Nagpur University, Nagpur, Maharashtra, India

Ritesh L. Kohale

Department of Physics, Sant Gadge Maharaj Mahavidyalaya, Hingna, Nagpur, Maharashtra, India

Sanjay J. Dhoble

Department of Physics, Rashtrasant Tukadoji Maharaj Nagpur University, Nagpur, Maharashtra, India

Hendrik C. Swart

Department of Physics, University of the Free State, Bloemfontein, South Africa

WP
WOODHEAD
PUBLISHING
An imprint of Elsevier

ELSEVIER

Notices
Knowledge and best practice in this field are constantly changing. As new research and experience broaden our understanding, changes in research methods, professional practices, or medical treatment may become necessary.

Practitioners and researchers must always rely on their own experience and knowledge in evaluating and using any information, methods, compounds, or experiments described herein. In using such information or methods they should be mindful of their own safety and the safety of others, including parties for whom they have a professional responsibility.

To the fullest extent of the law, neither the Publisher nor the authors, contributors, or editors, assume any liability for any injury and/or damage to persons or property as a matter of products liability, negligence or otherwise, or from any use or operation of any methods, products, instructions, or ideas contained in the material herein.

For information on all Woodhead Publishing publications visit our website at
https://www.elsevier.com/books-and-journals

Working together
to grow libraries in
developing countries

www.elsevier.com • www.bookaid.org

Contents

Synthesis and photoluminescence in Eu²⁺ activated alkali/alkaline earth halides and chlorophosphate blue phosphors

7

Chhagan D. Mungmode[1] *and Dhananjay H. Gahane*[2]
[1]M. G. Arts, Science & Late N. P. Commerce College, Armori, Maharashtra, India; [2]N.H. College, Bramhapuri, Maharashtra, India

7.1 Introduction

According to Nobel Laureate Richard Smalley, one of the most important problems, the world facing today is energy crisis. Light has played major role in the development of human civilization. The modern society heavily depends on how we produce and use energy. About 20% of total electricity is used for lighting purpose. Along with the production cost of the electrical energy, there is the environmental cost in the form of smog and CO_2 emission associated with electricity production.

The main source of lighting till the recent years was incandescent bulb which was discovered by Edison in 1879 [1]. In incandescent lighting, the filaments convert only about 5% of supplied energy into visible light whereas more than 95% is transferred into heat. The other significant source of lighting today is fluorescent bulbs/tubes which were introduced in 1939 by General Electrics [2]. In these devises, phosphor coated on inner layer of the tube is excited by ultraviolet radiation produced by mercury plasma maintained at low pressure. This source of light is most efficient for general purpose lighting but fluorescent tubes contains mercury which may cause health hazards if not properly disposed. New materials developed in 1960s which emits light by the conversion of electrical energy. This process includes excitation and deexcitation of electrons of the material at room temperature. These systems which are producing white light are termed solid-state lighting (SSL) [3]. These promising devices can replace conventional light sources, with impressive economic and environmental benefits.

White light using LED can be generated by two techniques: mixing red, green, blue (RGB) light in proper amount to get white light, and down-conversion of some emitted light by $In_xGa_{1-x}N$-based blue and nUV LED systems to get white light. This requires at least three components: each one generating red, green, and blue. Each of these components requires separate supply circuit to properly adjust intensity of each component to get white light. The another approach to produce white light is mixing blue and yellow light in proper amount [4,5].

7.2   Review of Eu^{2+} emission

Nowadays, white light can be obtained by properly mixing blue light emitted by GaN LED with yellow light emitted by inorganic phosphor like Ce^{3+} doped $Y_3Al_5O_{12}$ [6]. But, this combination gives bluish cold illumination instead of natural warm white light. To get illumination approximating natural warm white light, red emitting phosphor can be added to the system and the other way is to use Ultra Violet emitting LED in combination with three phosphors (blue, green and red). Phosphors synthesized by doping trivalent lanthanide ions in a host lattice are extensively studied and are being used in applications. One example is, red emitting Eu^{3+} doped Y_2O_3 phosphor used in mercury discharge lamp [7,8].

Electric dipole transitions $[Ye]4f^n \rightarrow [Ye]4f^n$ are forbidden in trivalent lanthanide ions and gives low quantum efficiencies. Due to this lanthanide with two valency may be used [9] as electric dipole $[Ye]4f^n \rightarrow [Ye]4f^{n-1}5\,d^1$ transitions are allowed which leads to higher intensities [10]. The energy position of 5d orbitals may change due to crystal field of host material as these energy levels are less shielded than 4f orbitals. Thus, we can tune the emission wavelength by doing favorable changes in host material. Divalent Europium can be easily stabilized as compared to other divalent lanthanides and emission wavelength belongs to visible spectrum. Therefore, many Eu^{2+} activated phosphors have been studied and many of these have found applications in SSL. $BaMgAl_{10}O_{17}$: Eu^{2+} (BAM) is well known commercial blue phosphor. Many silicon-based nitrides like $SrSi_2O_2N_2$:Eu^{2+} [11] or $M_2Si_5N_8$:Eu^{2+} (M = Sr, Ba) are being used in LED applications [12−14]. Dorenbos reviewed Eu^{2+} activated compounds till 2003 [15].

In this chapter, we have presented the preparation and photoluminescence characteristics of blue emitting Eu^{2+} doped alkali/alkaline earth halides and some chlorophosphate phosphors.

7.3   Synthesis of phosphor using wet chemical method

Most of the phosphors presented in this chapter are prepared by Wet-Chemical method and studied for photoluminescence. Wet-Chemical synthesis is simpler and cost-effective as compared to solid-state synthesis.

Most of the starting materials used were of analytical grade (AR) manufactured by Merck Ltd. Stoichiometric amounts of metal carbonates, Eu_2O_3 and other precursors were taken. Samples were prepared by dissolving these starting materials in halogen acid. The solution was then heated so that the extra acid gets boiled off and the solutions become dry. The resulting compound was further heated for 2 h at 475 K in air and crushed to get fine powder.

For example, stoichiometric amounts for synthesis of $(Ca_{1.98}\,Eu_{0.02})PO_4Cl$ are as follows:

Chemical	Molecular wt. A	Molar ratio B	Weight required for 1 mole C = A × B	Weight taken C/98.0882 (gm)
CaHPO$_4$	136.06	1	136.06	1.38711
CaCO$_3$	100.09	0.98	98.0882	1
Eu$_2$O$_3$	351.92	0.01	3.5192	0.03588
HCl	36.46	1	36.46	0.3717

Calculation for HCl to convert from gm to ml:

Specific gravity = 1.18 kg
Assay = 41%
1 mL HCl = 1.18 * 0.41 gm HCl = 0.4838 gm HCl
1 gm HCl = 2.066 mL HCl
0.3717 gm HCl = 0.7679 mL HCl.

Now the prepared phosphors annealed for 1 h at various temperatures ranging between 623 and 1075 K in a reducing atmosphere provided by burning charcoal. This treatment reduces europium to divalent state.

7.4 General features of Eu^{2+} in alkali halides

Eu^{2+} ions doped in an alkali halide crystal, usually replaces the host cation whose crystal field symmetry depends on the crystal lattice. The electron arrangement of Eu^{2+} ion in the ground state is $4f^7\,5s^2\,5p^6$. Completely filled $5s^2$ and $5p^6$ orbitals shielded the electrons in partially filled 4f shell from external [16]. Transition from $^8S_{7/2}$ state of $4f^7$ configuration to $4f^6\,5\,d^1$ configuration in Eu^{2+} gives rise to emission. The lowermost $4f^6\,5\,d^1$ levels is near 34,000 cm^{-1} and is labeled ^8H_J for the free ion. The transition from $^8S_{7/2}$ state of $4f^7$ configuration to $4f^6\,5\,d^1$ configurational states causes the absorption. In general these excitation bands of Eu^{2+} in ionic crystals are situated in the ultraviolet region [17]. Such transitions are dipole allowed, hence the intensity of these transitions is quite high [18]. The splitting of the fivefold orbital degeneracy of the d-energy level into a doubly degenerate (E_g) and a threefold degenerate (T_{2g}) energy levels are caused by the crystal field acting at the Eu^{2+} site. Coordination of the ligands (symmetry of the crystal field) decides the relative positions of (E_g) and (T_{2g}) energy levels [16−19]. The excitation of Eu^{2+} ion from level $4f^7$ [$^8S_{7/2}$] to the levels of $4f^6$ $5\,d^1$ configuration is associated with several broad and depends on crystal field strength.

According to an electrostatic model for the cubic crystalline field, the separation between E_g and T_{2g} energy levels is proportional to R^{-5}, where R is the distance between the impurity ion and its surrounding ligands. The values of splitting between E_g and T_{2g} energy levels go on increasing from iodides to oxides in the following sequence [20].

Free ion $< I^- < Br^- < Cl^- < S^{2-} < F^- < O^{2-}$

Hence, redshift in the emission spectra is observed going from iodide to oxides phosphors. Single broad band emission spectra are observed in many of the Eu^{2+} doped alkali halides due to nonradiative decay from the excited state E_g to T_{2g} and radiative decay from T_{2g} state to the ground state.

7.5   Result and discussion

7.5.1   *Photoluminescence in Cs₂MCl₄:Eu²⁺ (M = Ba, Ca) phosphor*

Appleby et al. [21] studied Cs_2BaBr_4, Rb_2BaBr_4, Cs_2BaCl_4, and Rb_2BaCl_4 phosphors for their structure. These phosphors are also studied for PL and PSL. The method of synthesis of these materials is conventional solid state route which takes long time. Recently, Gahane et al. reported synthesis of Eu^{2+} activated $ABCl_3$ type hosts like $KSrCl_3$ by wet chemical method and studied luminescence [22]. Eu^{2+} emission in all $ABCl_3$ type chlorides is very intense as compared to commercially available $BaMgAl_{10}O_{17}:Eu^{2+}$ (BAM).

In this section, we discuss the synthesis and photoluminescence of Eu^{2+} activated Cs_2BaCl_4 and Cs_2CaCl_4 phosphor using wet-chemical method.

7.5.1.1   *Cs₂BaCl₄:Eu²⁺*

Ternary halide Cs_2BaCl_4 crystalizes in body centered cubic structure (Th_3P_4 type) (Fig. 7.1), having space group I—43d (220), where Th sites (12a) are occupied by Cs and Ba cations randomly in the 2:1 ratio [21], whereas (16c) is the site occupied by the halide atoms.

Fig. 7.2 (curve b) shows photoluminescence excitation spectra of $Cs_2(Ba_{0.99}Eu_{0.01})$ Cl_4 for 440 nm emission. The excitation spectra include several unresolved bands that cover wavelengths from UV to visible; the bands around 280 and 340 nm are most prominent. Therefore, radiations of the near ultraviolet (nUV) rays are efficiently used to excite $Cs_2BaCl_4:Eu^{2+}$. Fig. 7.2 (curve a) presents PL emission spectrum of $Cs_2(Ba_{0.99}Eu_{0.01})Cl_4$ phosphor quenched at 723 K. Photoluminescence spectra show the emission in blue region with Full Width at Half Maxima (FWHM) equal to 53.1 nm. High intensity blue emission peaking at 443 nm is obtained for 1 nm slit width of spectrometer when phosphor is excited by 365 nm light.

Emission spectra are due to dipole allowed $4f^6 5d^1 \rightarrow 4f^7$ de-excitation of Eu^{2+} dopant ion present in halide crystal [23]. Highly intense PL spectra may be due to
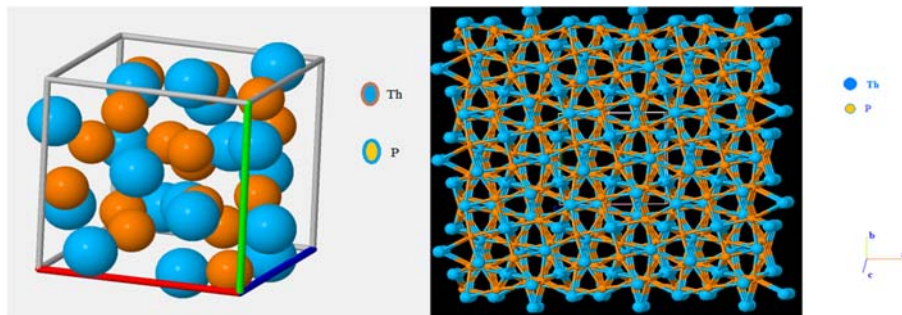

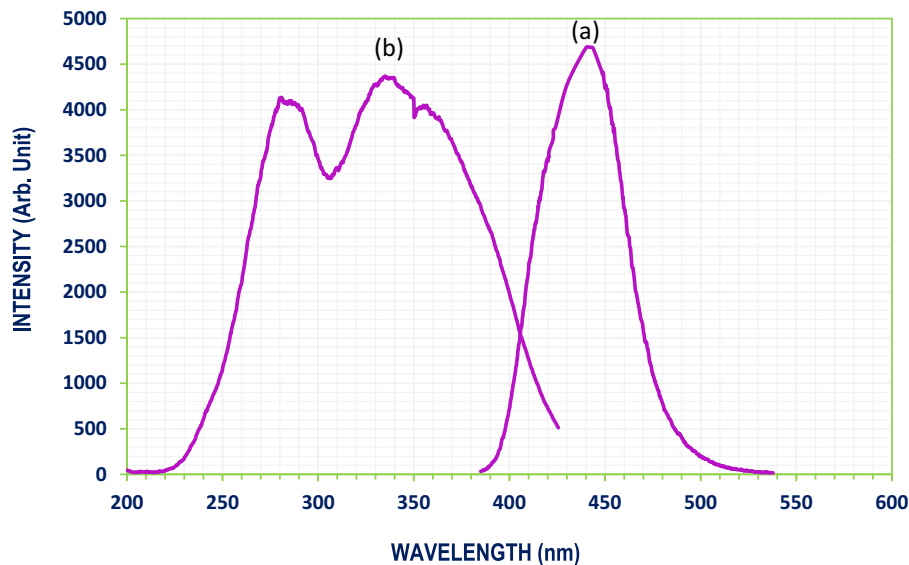**Figure 7.1** Unit cell and crystal structure of Th_3P_4.

Figure 7.2 Photoluminescence spectrum of $Cs_2(Ba_{0.99}Eu_{0.01})Cl_4$. (a) Emission spectra of $Cs_2(Ba_{0.99}Eu_{0.01})Cl_4$ under 365 nm excitation. (b) Excitation spectra of $Cs_2(Ba_{0.99}Eu_{0.01})Cl_4$ for 440 nm emission.

lower symmetry of the crystal. Emission peak observed in present work (443 nm) matches well with the reported value (441 nm) [21].

7.5.1.2 $Cs_2CaCl_4{:}Eu^{2+}$

Cs_2CaCl_4 belongs to high—T_c cuprate family. Fig. 7.3 presents photoluminescence spectrum of $Cs_2(Ca_{0.995}Eu_{0.005})Cl_4$ phosphor. The emission spectra of $Cs_2(Ca_{0.995}Eu_{0.005})Cl_4$ phosphor annealed at different temperature are shown by curve a, b and c in Fig. 7.3. Increasing the annealing temperature up to 875 K causes an increase in emission intensity and then after it decreases as shown in inset. Upon being excited by 365 nV radiations, phosphor reduced at 875 K reveals a maximum intensity of PL centered around 446 nm. This emission has a width of 21 nm (FWHM). Increasing the annealing temperature from 675 to 975 K results in a blue shift from 448.5 to 440 nm. This may possibly because of increase in crystal field splitting due to increased crystallinity with increasing annealing temperature. Single emission peak signifies the phase purity of the phosphor. Fig. 7.3 (curve d) presents excitation spectrum of $Cs_2(Ca_{0.995}Eu_{0.005})Cl_4$. The most prominent bands in the vicinity of UV region are seen around 360 and 380 nm. In conclusion, phosphor can be efficiently excited by nUV radiation, proving its overall suitability as a blue component for near UV LEDs.

There is a small redshift in the emissions maxima from 443 nm for $Cs_2(Ba_{0.99}Eu_{0.01})Cl_4$ to 446 nm for $Cs_2(Ca_{0.995}Eu_{0.005})Cl_4$ upon excited by 365 nm

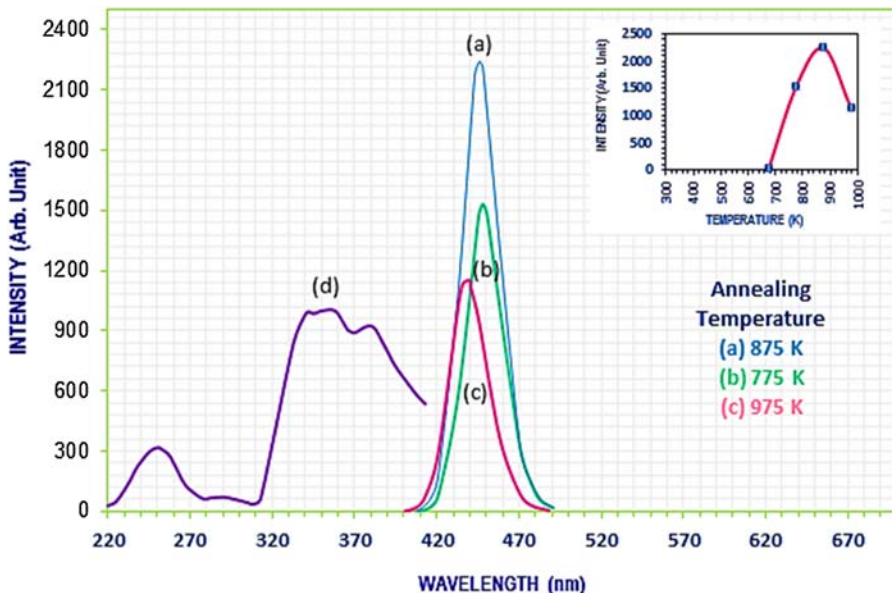**Figure 7.3** Photoluminescence spectrum of $Cs_2(Ca_{0.995}Eu_{0.005})Cl_4$ phosphor. (a)−(c) Emission spectra of $Cs_2(Ca_{0.995}Eu_{0.005})Cl_4$ under 365 nm excitation. (d) Excitation spectra of $Cs_2(Ca_{0.995}Eu_{0.005})Cl_4$ for 440 nm emission. Inset: Variation of the emission intensity with annealing temperature (K).

radiation. This is due to Ca atoms are substituted for Ba atoms and this results in an increased crystal field splitting.

.

7.5.2 Photoluminescence in NaCa$_2$Br$_5$:Eu^{2+} phosphor

$NaCa_2Br_5$ phosphor is prepared by wet-chemical method. Stoichiometric amounts of $NaCO_3$, $CaCO_3$, Eu_2O_3 and HBr were taken as starting materials. $NaCa_2Br_5$ crystallizes in orthorhombic (space group Pnma) crystal system (Fig. 7.4) [24,25]. Fig. 7.5 (curve b) presents the PL excitation spectrum of Eu^{2+} activated $NaCa_2Br_5$ phosphor. There are unresolved bands in the excitation band due to the $4f^65d^1$ multiplets of Eu^{2+} excited states. It is characterized by two prominent peaks around 275, 338 nm and a shoulder around 370 nm is also observed attributable by Eu^{2+}. As a result, it has a significant response across the entire UV spectrum.

Fig. 7.5 (curve a) presents photoluminescence emission spectrum of Eu^{2+} activated $NaCa_2Br_5$ phosphor for 1 nm slit width. An intense blue emission spectrum is obtained for $NaCa_{1.98}Br_5:Eu^{2+}_{0.02}$ quenched from 775 K under 365 nm excitation. A peak in broad band emission can be seen at 439 nm in the emission spectra corresponding to $4f^65d \rightarrow {}^8S$ allowed electric dipole transition. Since the phosphor was hygroscopic and XRD facility was not easily available, XRD characterization was not carried out. No reference is found for photoluminescence of $NaCa_2Br_5:Eu^{2+}$ in the literature for
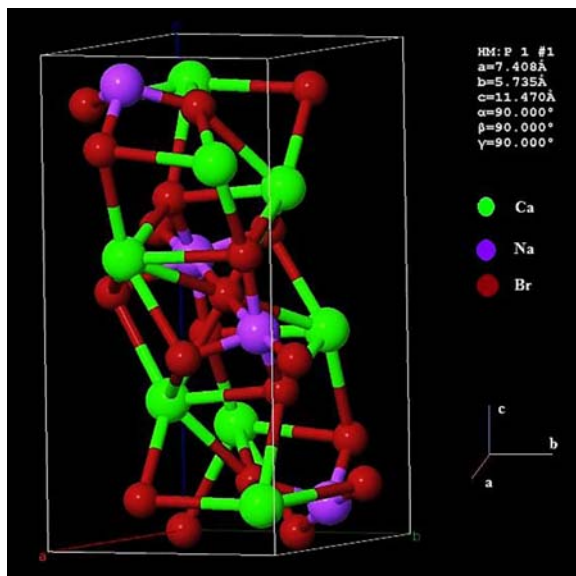
Figure 7.4 Unit cell of $NaCa_2Br_5$.

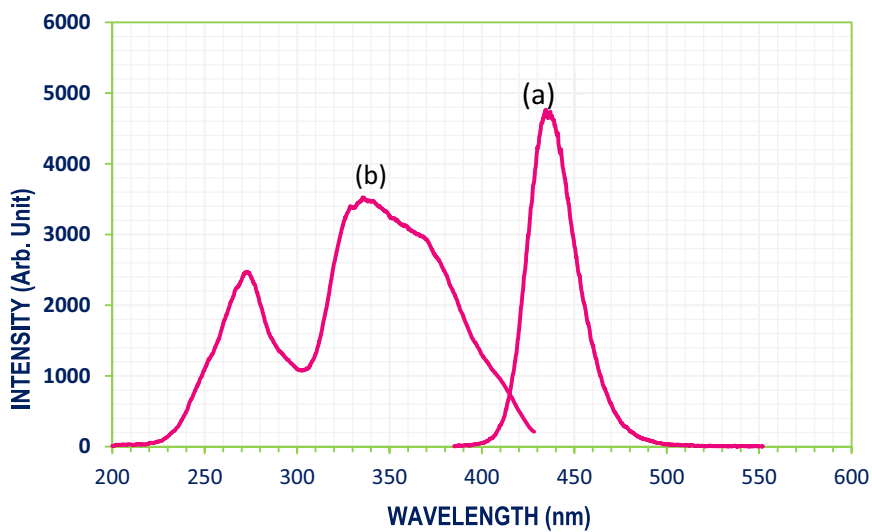**Figure 7.5** Photoluminescence spectrum of Eu^{2+} activated $NaCa_2Br_5$ phosphor. (a) Emission spectra of $NaCa_2Br_5$: Eu^{2+} for 365 nm excitation. (b) Excitation spectra of $NaCa_2Br_5$: Eu^{2+} for 435 nm emission.

comparison. Consequently, this could be the first report regarding the Eu^{2+} activated host. Thus, the luminescence is highly efficient due to the small Stoke's shift.
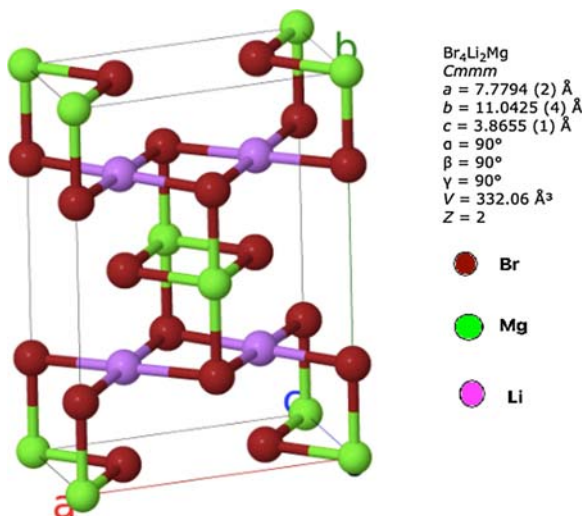
7.5.3   Photoluminescence in Eu^{2+} activated $Li_xMgM_{(x+2)}$ (x = 2, 6; M = Br, Cl) phosphors

In a review of recent luminescence studies on Eu^{2+} [15], it was found that there have been very few studies on bromides. According to a report Li_2MgBr_4:Ce may be used as neutron scintillation detector but no report on Eu^{2+} activated Li_xMgM_{x+2} (x = 2, 6; M = Br, Cl) has found. The lack of luminescence evidence prompted our investigation of Eu^{2+} in Li_xMgM_{x+2}.

Li_2MgBr_4 is isostructural with Mn_2SnS_4. The crystallization occurs in the orthorhombic space group Cmmm with Z = 2 (a = 777.94 (2), b = 1104.25 (4), c = 386.55 (1)) (Fig. 7.6) and undergoes a phase transition to the cubic structure above 575 K [26]. Despite being much bigger than Mg^{2+}, Eu^{2+} can be incorporated only at the Mg^{2+} substitution sites.

Data on the PL of Li_2MgBr_4 is presented in Fig. 7.7. An intense, violet-blue emission is observed for $Li_2Mg_{0.99}Eu_{0.01}Br_4$ annealed at 850 K when excited by 365 nm radiation (curve a). The emission band peaks at 430.8 nm and have half intensity wavelengths corresponds to 451.2 and 416 nm having emission bandwidth (FWHM) 35.2 nm. The excitation band (curve b) has several unresolved bands covering entire nUV region extends up to visible region. Observations around 365 nm show prominent bands in conjunction with a shoulder at 260 nm, inferring transition from the ^8S ground state of $4f^7$ to a $4f^6 5d^1$ state. Li_6MgBr_8 crystallizes in cubic space group $Fm\overline{3}m$ (Z = 4), A structure of type Mg_6MnO_8 with the Mg atom on a site with 4m symmetry (Wyckoff site 4a) and the Br atom on a site with 8c symmetry (Wyckoff site c) (Fig. 7.8). Compounds of this type represent an ordered defect variant of the NaCl structure (Suzuki-type) [27].
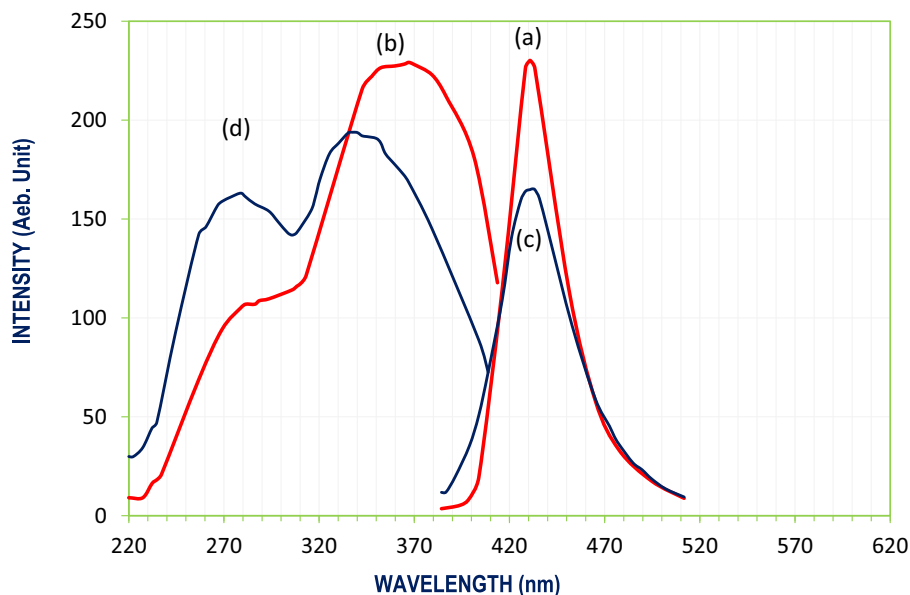
Figure 7.6 Unit cell of Li_2MgBr_4.

Br₄Li₂Mg
Cmmm
a = 7.7794 (2) Å
b = 11.0425 (4) Å
c = 3.8655 (1) Å
α = 90°
β = 90°
γ = 90°
V = 332.06 Å³
Z = 2

● Br
● Mg
● Li

Figure 7.7 PL spectra for Li_2MgBr_4:Eu^{2+} and Li_6MgBr_8:Eu^{2+}. (a) Emission in Li_2MgBr_4:Eu^{2+} for 365 nm excitation. (b) Excitation for 430.8 nm emission. (c) Emission in Li_6MgBr_8:Eu^{2+} for 365 nm excitation. (d) Excitation for 430 nm emission.

Data on the PL of Li_6MgBr_8 presented in Fig. 7.7. A weak, broad band blue emission compare to Li_2MgBr_4 is observed for $Li_6Mg_{0.99}Eu_{0.01}Br_8$ annealed at 850 K when excited by nUV 365 nm radiation (curve c). At 430 nm, there is maximum emission. It
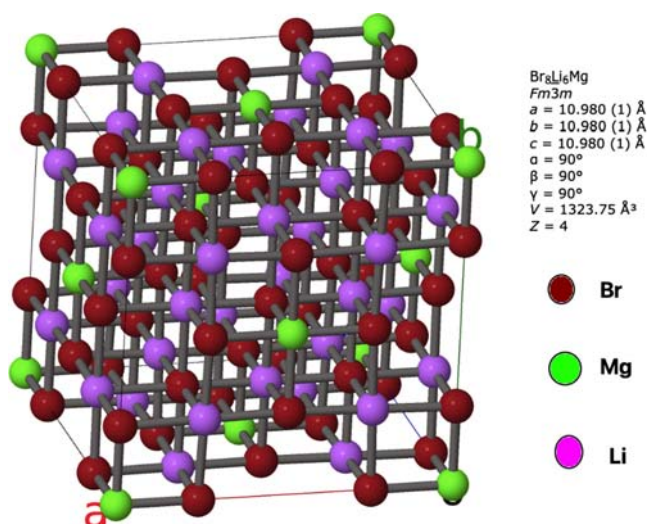

Figure 7.8 Unit cell of Li_6MgBr_8.

has spectral width (FWHM) of 46 nm. There are two bands with 277 and 337 nm in the excitation spectrum of this phosphor, which is broad band from 250 to 400 nm (curve d). No reference on photoluminescence of Eu^{2+} activated Li_2MgBr_4 and Li_6MgBr_8 is found for the comparison. Hence, this may be the first report.

Ternary lithium chloride Li_2MgCl_4 crystalizes in space group Fd3m (with $z = 8$) of an inverse spinel structure type [28]. Fig. 7.9 (curve a) shows the photoluminescence excitation spectrum of Eu^{2+} activated Li_2MgCl_4 phosphor. The excitation spectrum is characterized by peaks around 271, 328 nm and a shoulder around 330 nm is also observed which is attributed to Eu^{2+} excitation in host lattice. Hence, the phosphor shows a good response throughout UV region. Fig. 7.9 (curve b) presents the PL emission spectra for $Li_2MgCl_4:Eu^{2+}$ (1 mol%) quenched from 724 K. Emission slit width was set at 1 nm. Upon 320 nm excitation, emission spectra show broad blue band centered around 435 nm corresponding to a $4f^65d \rightarrow {}^8S$ electric dipole allowed transition.

Fig. 7.10 (curve b) shows the photoluminescence excitation spectrum and Fig. 7.10 (curve a) shows emission spectrum for $Li_6MgCl_8:Eu^{2+}$. The excitation spectrum covers entire nUV region and characterized by peaks around 269 nm, 332 nm and a shoulder around 370 nm. Fig. 7.10 (curve a) shows emission spectra for
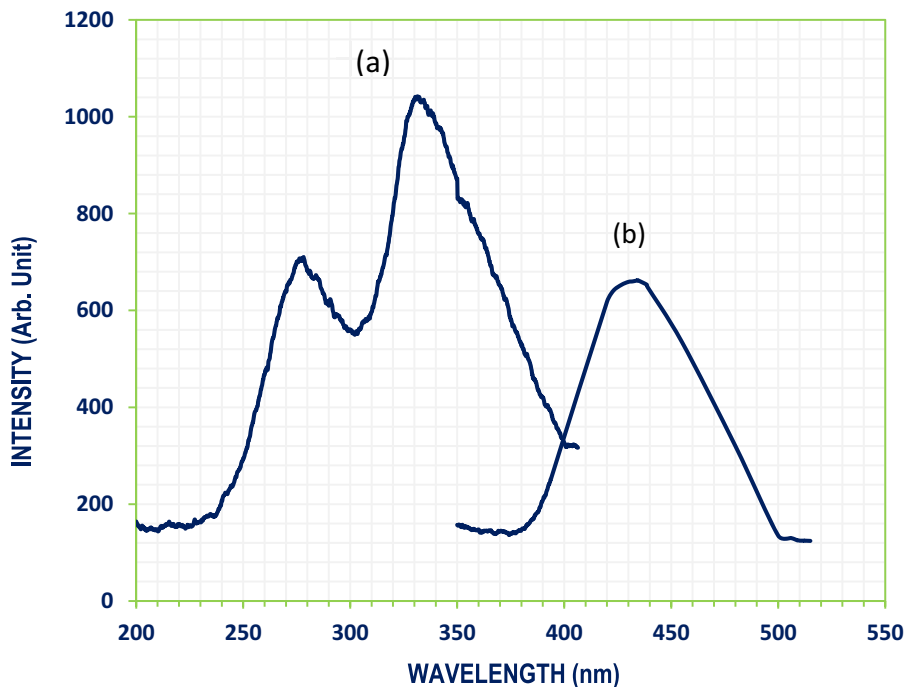

Figure 7.9 Photoluminescence spectrum of $Li_2MgCl_4:Eu^{2+}$ phosphor. (a) Excitation spectra of $Li_2MgCl_4:Eu^{2+}$ for 430 nm emission. (b) Emission spectra of $Li_2MgCl_4:Eu^{2+}$ for 320 nm excitation.
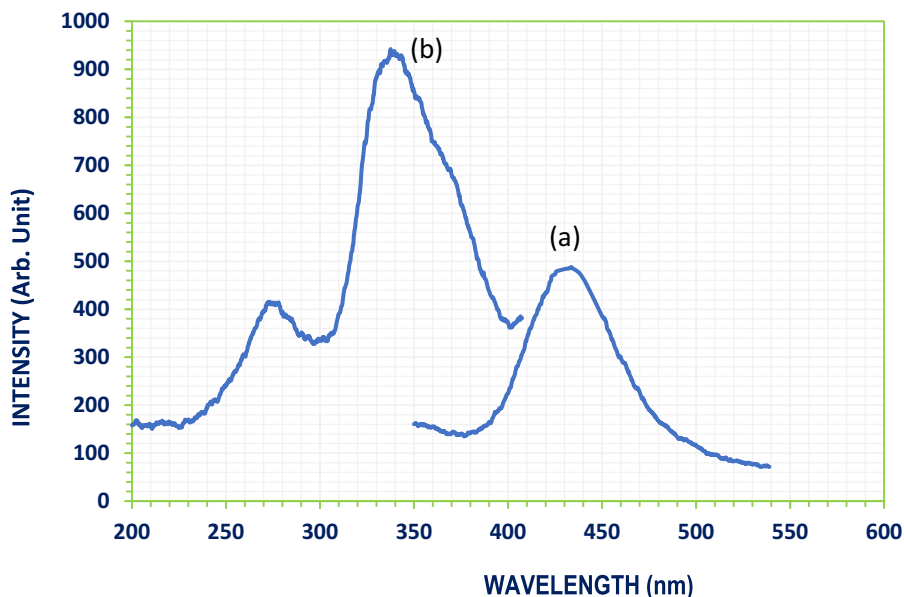
Figure 7.10 Photoluminescence spectrum of $Li_6MgCl_8:Eu^{2+}$ phosphor. (a) Emission spectrum of $Li_6MgCl_8:Eu^{2+}$ for 320 nm excitation. (b) Excitation spectra of $Li_6MgCl_8:Eu^{2+}$ for 430 nm emission.

$Li_6MgCl_8:Eu^{2+}$ (1 mol%) quenched from 724 K under 320 nm excitation. A broad band emission peak is observed for a slit width of 1 nm at 434 nm.

$Li_xMgCl_{(x+2)}$ (x = 2, 6) has never been reported before. Accordingly, this is likely the first report on Eu^{2+} activated $Li_xMgCl_{(x+2)}$. It was observed that PL emission peaks are slightly red shifted for both Eu^{2+} activated $Li_xMgCl_{(x+2)}$ compare to $Li_xMgBr_{(x+2)}$. The PL emission intensity was also found to decreases for x = 6 as compared to x = 2. Decrease in intensity may be due to decreased crystallinity. These phosphors shows excellent response in nUV region. $Li_xMgM_{(x+2)}$ (x = 2, 6; M = Br, Cl) phosphors are promising blue emitters for LED application.

7.5.4 Photoluminescence in Eu^{2+} activated CaI_2

Hofstadter et al. [29] reported CaI_2 and CaI_2 (Eu) scintillation Crystals. CaI_2 crystals doped with Eu^{2+}, Gd^{2+}, Tl^+, Pb^{2+}, and Mn^{2+} demonstrate recombination luminescence in an additional report [30]. CaI_2 activated with Eu^{2+} has been shown for the first time to emit efficient luminescence in recent work [31]. The emission intensity was comparable to commercially available phosphor (BAM, Sylvania 2466 blue). This earlier work did not examine the effect of annealing temperature on PL emission. In the present work, effect of annealing temperature and doping concentration of Eu^{2+} on the emission spectra of CaI_2 is presented.

CaI_2 crystallizes as a trigonal space group $Pm\overline{3}1$ (Fig. 7.14). The distinction within the ionic radii of Ca^{2+} and Eu^{2+} is comparatively less and CaI_2 will accommodate additional Eu^{2+} [31].

Formation of CaI_2 compound is confirmed using XRD analysis of the phosphor in previous work done by Gahane et al. [31]. Fig. 7.11 shows Eu^{2+} emission and excitation spectra of $(Ca_{1-x}Eu_x)I_2$ where x is doping concentration of Eu^{2+}. The wavelength range from UV to visible is covered by a broad excitation spectrum (curve d). It is made up of many overlapping bands in the near UV range between 360 and 410 nm, as well as two smaller bands around 260 and 285 nm. At x = 0.005 (curve c), there is less blue emission. Highest emission intensity is observed for x = 0.01 (curve a) as compared to x = 0.02 (curve b) and x = 0.005. Upon excited with 365 nm light, $Ca_{0.99}Eu_{0.01}I_2$ phosphor shows emission maximum centered at 462 nm annealed at 873 K. The intensity of emission spectra is comparable to that of $(BaMgAl_{10}O_{17}:Eu^{2+})$. The observed emission maximum agrees well with the published value [30]. As indicated in Fig. 7.11, concentration quenching was found for both greater and lower concentrations. Further, $Ca_{0.99}Eu_{.01}I_2$ was annealed at various temperatures in reducing atmosphere and PL spectra were investigated. Fig. 7.12 presents PL emission spectra of $Ca_{0.99}Eu_{0.01}I_2$ as a function of annealing temperature. From the curves a, b, c, d, e corresponding to 623, 773, 873, 923, 973 K, respectively, it is observed that highest PL emission intensity is obtained for the sample annealed at temperature 923 K in reducing atmosphere as compared to other annealing temperature. The emission intensity goes on increasing up to temperature 923 K and decrease for higher temperature as shown in Fig. 7.13. Therefore, temperature quenching is occur above and below 923 K. CIE (1931) chromaticity diagram is presented in Fig. 7.15. The chromaticity coordinates for 462 nm emission wavelength of $Ca_{0.99}Eu_{0.01}I_2$ phosphor are x = 0.1400, y = 0.0399. When compared to

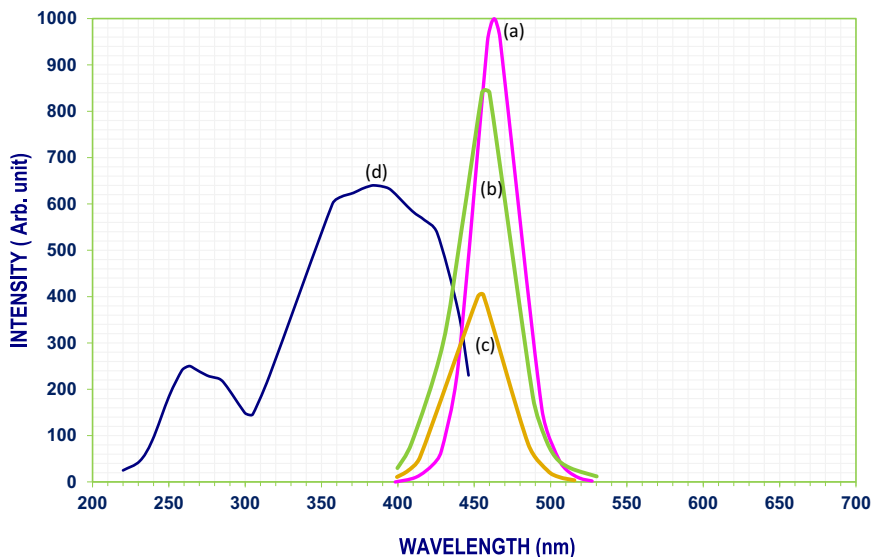**Figure 7.11** Photoluminescence spectra of $CaI_2:Eu^{2+}$ for different concentration of Eu^{2+}. (a) $Ca_{0.99}:Eu_{0.01}I_2$ (b) $Ca_{0.98}:Eu_{0.02}I_2$ (c) $Ca_{0.995}:Eu_{0.005}I_2$ (d) excitation spectra.

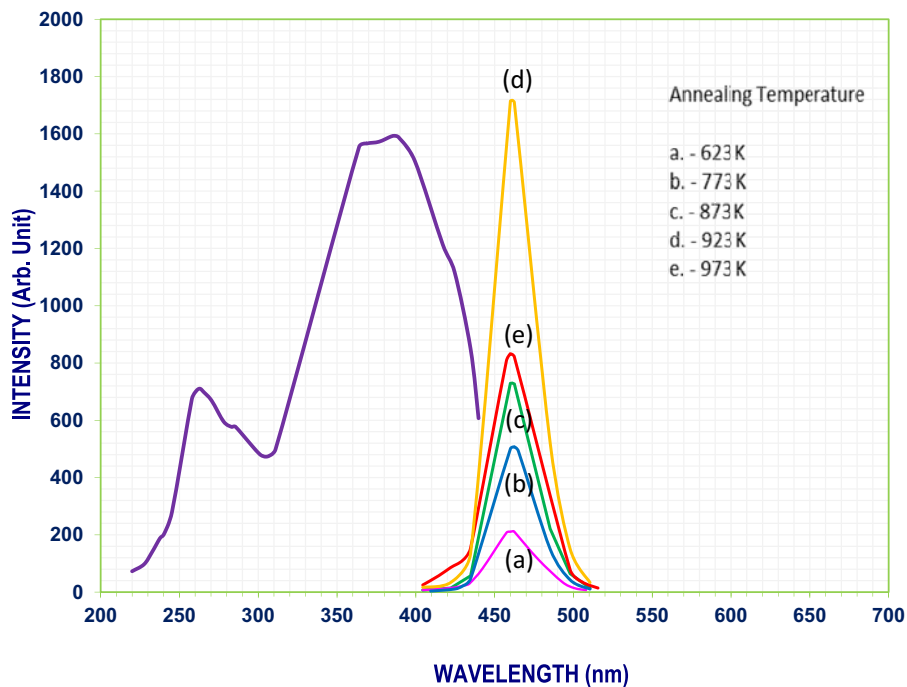**Figure 7.12** Photoluminescence spectra of $Ca_{0.99}:Eu_{0.01}I_2$ phosphor annealed at different temperature.
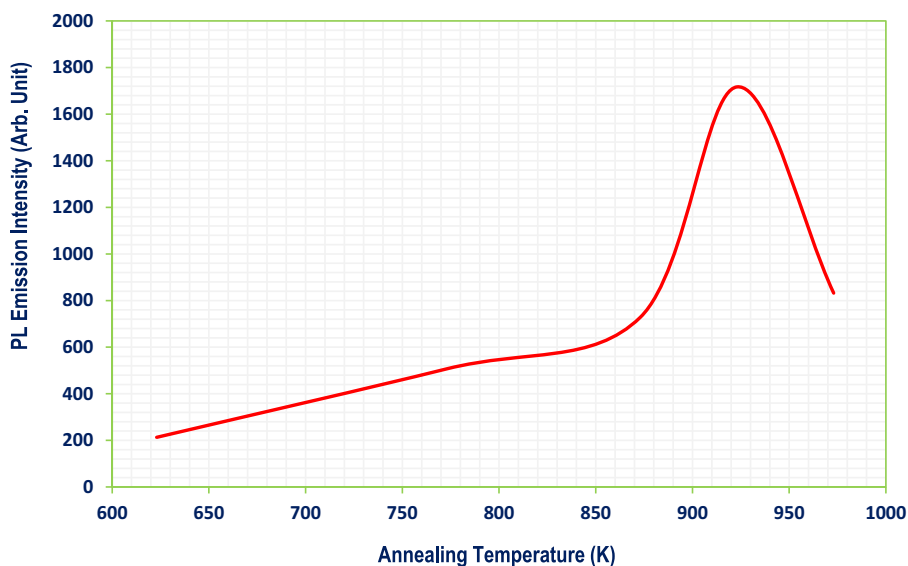

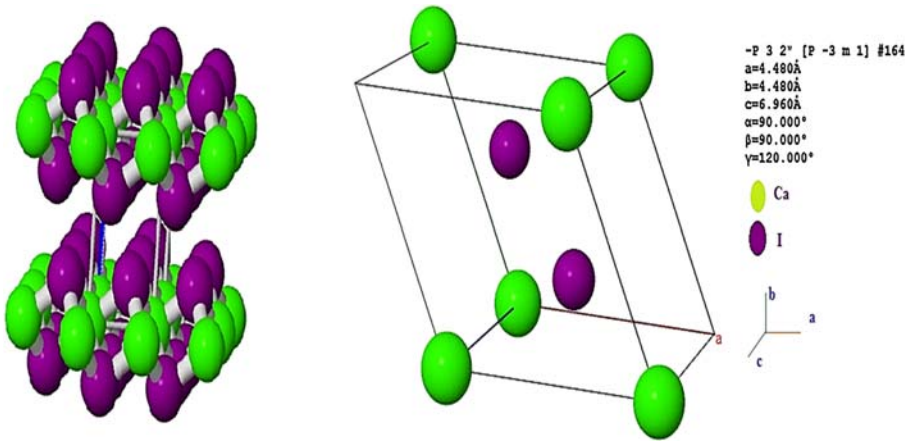**Figure 7.13** Variation of PL Emission intensity as a function of annealing temperature.

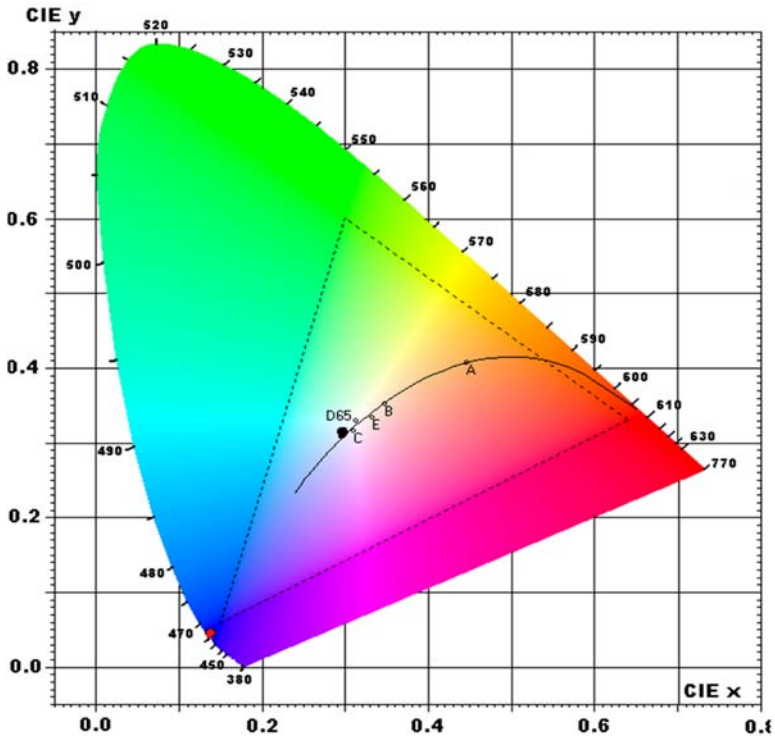**Figure 7.14** Crystal structure and unit cell of CaI_2.

Figure 7.15 CIE chromatic coordinates of $Ca_{0.99}Eu_{0.01}I_2$.

commercially available $BaMgAl_{10}O_{17}$:Eu^{2+} phosphor for 453 nm emission wavelength, the CIE value of prepared phosphor is better (x = 0.144, y = 0.089) [32]. It indicates that CaI_2:Eu^{2+} is promising blue component nUV−based white LED.

7.5.5 Synthesis and photoluminescence in $(CaBa_{0.96})PO_4Cl:_{0.04}Eu^{2+}$

Phosphates have an optical absorption edge with a relatively short wavelength. As a result, they're good hosts for active rare earth (RE) ions [33]. Alkaline earth halophosphates were identified as effective ultraviolet stimulable luminous materials by McKeag and Ranby in 1942 [34]. Halophosphates of alkaline earth metals with a general molecular formula $M_5(PO_4)_3X$ (M = Ca, Sr, Ba; X = Cl, Br, F, OH) are widely recognized for their uses as phosphor materials [35,36], laser hosts [37], and biocompatible materials [38]. Their usage in the LED technology in England and the US soon established them as a significant class of chemicals [39−42]. These halophosphates have been the topic of extensive theoretical and experimental research since then. Johnson has combed through a large amount of literature amassed over the last 60 years [43]. However, it has been observed that the majority of these effective phosphate phosphors are made using the traditional high-temperature solid-state reaction approach, which necessitates meticulous grinding and a lengthy synthesis time.

Wet chemical synthesis of $(CaBa_{0.96})PO_4Cl:_{0.04}Eu^{2+}$ phosphor is used in this study by substituting Ba ions in place of Ca ions in Ca_2PO_4Cl phosphor and studied its photoluminescence spectra.

Sample is prepared by dissolving stoichiometric amounts of $CaHPO_4$, $BaCO_3$, and Eu_2O_3 into HCl. The leftover acid was then heated away, and the solution was evaporated until it was completely dry. The resultant material was dried in air for 2 h at 475 K, then crushed into fine powders and annealed for 1 h at 1073 K in a reducing environment created by burning charcoal to reduce the activator to a divalent state.

Fig. 7.16a presents PL emission spectra of $(CaBa_{0.96})PO_4Cl:_{0.04}Eu^{2+}$ phosphor. An intense broad band blue emission is observed peaking at 461 nm when excited by 337 nm nUV light. The emission characteristic of the sample is attributable to $4f^6 5d^1$ to $4f^7$ transition of Eu^{2+} ion. The FWHM is found to be 71 nm. Fig. 7.16b shows excitation spectrum of $(CaBa_{0.96})PO_4Cl:_{0.04}Eu^{2+}$ for 450 nm emission. A broad band excitation covers UV region up to visible region. Multiple overlapping bands near the UV range of 250−430 nm make up the excitation spectrum. As a result, nUV light can effectively excite the phosphor. No previous report on this phosphor is found, hence this could be the first report.

7.5.6 Synthesis and photoluminescence in Eu^{2+} activated $Sr_{2.54}Ba_{2.45}(PO_4)_3Cl$

$Sr_5(PO_4)_3Cl$ is well-known blue emitting phosphor [36]. However, photoluminescence in $Sr_{2.54}Ba_{2.45}(PO_4)_3Cl$:$Eu^{2+}$ is not found. $SrHPO_4$, $SrCO_3$, $BaCO_3$, $(NH_4)_2HPO_4$, and Eu_2O_3 are dissolved in HCl and used to make the sample. The excess acid was then heated away, and the solutions were evaporated until they were completely dry. The
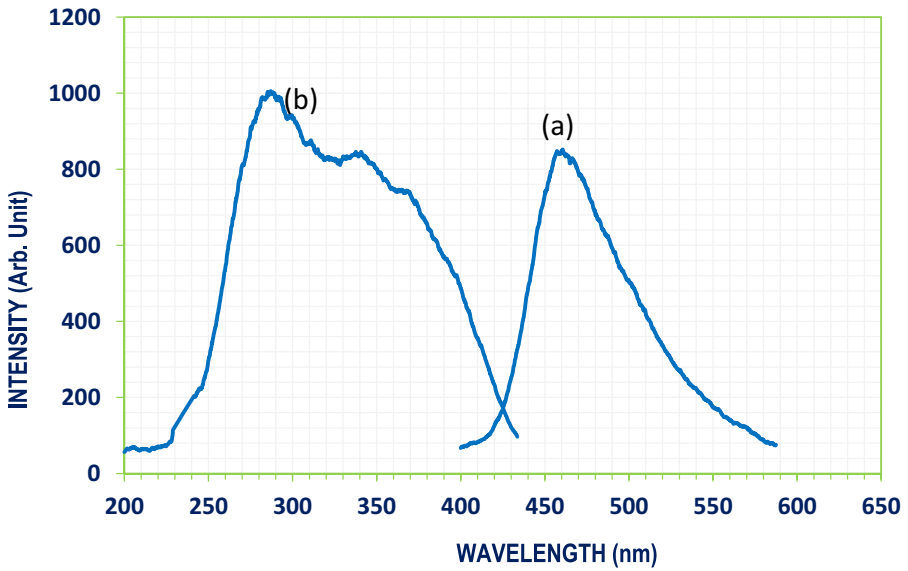
Figure 7.16 (a) PL emission spectra of $(CaBa_{0.96})PO_4Cl:_{0.04}Eu^{2+}$ for 337 nm excitation. (b) Excitation spectra of $(CaBa_{0.96})PO_4Cl:_{0.04}Eu^{2+}$ for 450 nm emission.
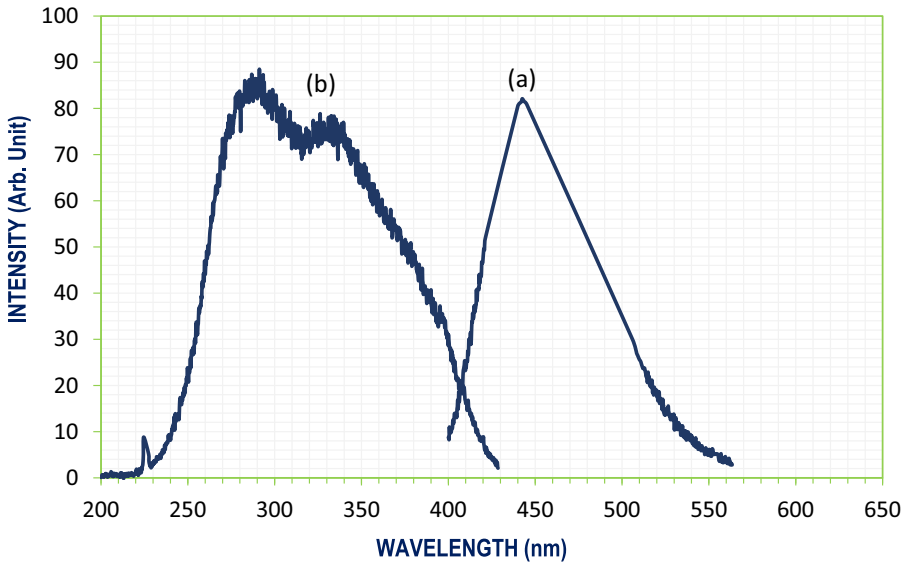
Figure 7.17 PL spectra for Eu^{2+} activated $Sr_{2.54}Ba_{2.45}(PO_4)_3Cl:Eu^{2+}$ (1 mol%). (a) Emission in $Sr_{2.54}Ba_{2.45}(PO_4)_3Cl:Eu^{2+}$ for 337 nm excitation. (b) Excitation of $Sr_{2.54}Ba_{2.45}(PO_4)_3Cl:Eu^{2+}$ for 450 nm emission.

powder was then dried in the air at 475 K for 2 h to get fine powders. To convert Europium to a divalent state, the powder was annealed at 1023 K for 1 h in a reducing environment created by burning charcoal.

Fig. 7.17a shows PL emission spectrum of $Sr_{2.54}Ba_{2.45}(PO_4)_3Cl:Eu^{2+}$ (1 mol%) annealed at 1023 K. A broad band emission centered at 443 nm is observed when excited by 337 nm light. The emission width is found to be 77 nm. Again, no report is found to compare the result of $Sr_{2.54}Ba_{2.45}(PO_4)_3Cl:Eu^{2+}$. Therefore, this may be the first report. Fig. 7.17b presents PL excitation spectrum of $Sr_{2.54}Ba_{2.45}(PO_4)_3Cl:Eu^{2+}$ (1 mol%). The excitation spectrum is characterized by two prominent bands centered around 290 and 335 nm. This demonstrates that nUV radiations may efficiently excite phosphor.

7.6 Conclusion

Photoluminescence data of prepared phosphors is presented in following table.

Phosphor	Eu^{2+} concentration (mol%)	Annealing temp (K)	Emission maxima (nm)	FWHM (nm)
Cs_2CaCl_4	0.5	875	446	21
Cs_2BaCl_4	1	723	443	53.1
$NaCa_2Br_5$	1	775	439	31
Li_2MgBr_4	1	850	430.8	35.2
Li_6MgBr_8	1	850	430	46
Li_2MgCl_4	1	724	435	70
Li_6MgCl_8	1	724	434	62
CaI_2	1	873	462	32
CaI_2	1	923	462	32
$CaBa_{0.96}Eu_{0.04})PO_4Cl$	2	1073	461 nm	71 nm
$Sr_{2.54}Ba_{2.45}(PO_4)_3Cl$	1	1023	443 nm	77 nm

The wet chemical approach is used to make all of these phosphors. Novel phosphors Cs_2CaCl_4 and $NaCa_2Br_5$ showed highly intense blue emission when excited by nUV light. The photoluminescence emission in Li_xMgCl_{x+2} is weak and broad band compared to Li_xMgBr_{x+2}; however, the emission wavelength shifts toward higher wavelength side. The doping concentration for CaI_2 is optimized as 1 mol% of Eu^{2+}. Maximum emission intensity for CaI_2 is observed at 923 K annealing temperature $(CaBa_{0.96})PO_4Cl:_{0.04}Eu^{2+}$ and $Sr_{2.54}Ba_{2.45}(PO_4)_3Cl:Eu^{2+}$ phosphors show blue emission. nUV light may effectively excite these phosphors. As a result, these phosphors are excellent candidates for use in SSL as a blue component.

References

[1] T.A. Edison, U.S. Patent No. 223 898, 1879.

[2] R.N. Thayer, B.T. Barnes, J. Opt. Soc. Am. 29 (1939) 131.

[3] Report of Basic the Energy Science Workshop on Solid State Lighting, US Dept. of Energy, Washington DC, USA, May 2006, p. 22.

[4] W.D. Collins, M.R. Krames, G.J. Verhoeckx, N.J.M. van Leth, US Patent 6,642,652, 2003.

[5] Y. Shimizu, K. Sakano, Y. Noguchi, T. Moriguchi, US Patent 5,998,925, 1999.

[6] S. Nakamura, G. Fasol, The Blue Laser Diode, Springer, Berlin, Germany, 1997.

[7] N.C. Chang, J.B. Gruber, J. Chem. Phys. 41 (10) (1964) 3227.

[8] T. Jüstel, H. Nikol, C. Ronda, Angew. Chem. Int. Ed. 37 (22) (1998) 3084−3103.

[9] A. García Fuente, et al., Chem. Phys. Lett. 622 (2015) 120−123.

[10] H.A. Höppe, Angew. Chem. Int. Ed. 48 (20) (2009) 3572−3582, https://doi.org/10.1002/anie.200804005.

[11] V. Bachmann, T. Jüstel, A. Meijerink, C. Ronda, P.J. Schmidt, J. Lumin. 121 (2) (2006) 441−449.

[12] Y.Q. Li, et al., J. Alloys Compd. 417 (2006) 273.

[13] X. Piao, T. Horikawa, H. Hanzawa, K.-I. Machida, Appl. Phys. Lett. 88 (2006), 161908-1.

[14] H.A. Höppe, H. Lutz, P. Morys, W. Schnick, A.J. Seilmeier, Phys. Chem. Solids 61 (2000) 2001.

[15] P. Dorenbos, J. Lumin. 104 (4) (2003) 239−260.

[16] J. Sugar, N. Spector, J. Opt. Soc. Am. 64 (1974) 1484.

[17] J.A. Hernanadez, F.J. Lopez, H.S. Murrieta, J.O. Rubio, J. Phys. Soc. Japan 50 (1) (1981) 225−229.

[18] S. Sugano, Y. Tanabe, H. Kanimura, Multiplets of Transition Metal Ions in Crystals, Academic Press, New York, USA, 1970.

[19] S. Bodyl, Mineralogia 40 (1−4) (2009) 85−94.

[20] M. Orichin, H.H. Jaffe, G. Kuehnlenz, Symmetry, Orbitals and Spectra, Wiley-Interscience, New York, USA, 1971.

[21] G.A. Appleby, A. Edgar, G.V.M. Williams, J. Appl. Phys. 96 (2004) 6281.

[22] D.H. Gahane, P.D. Dissertation, RTM Nagpur University, Nagpur, 2010.

[23] G. Blasse, B.C. Grabmaier, Luminescent Materials, Springer-Verlag, Berlin, Germany, 1994.

[24] A. Jain, S.P. Ong, G. Hautier, W. Chen, W.D. Richards, S. Dacek, S. Cholia, D. Gunter, D. Skinner, G. Ceder, K.A. Persson, Apl. Mater. 1 (1) (2013) 011002, https://doi.org/10.1063/1.4812323.

[25] G. Hautier, C. Fischer, V. Ehrlacher, A. Jain, G. Ceder, Inorg. Chem. 50 (2011) 656, https://doi.org/10.1021/ic102031h.

[26] M. Schneider, P. Kuske, H.D. Lutz, Z. Naturforsch, Chem. Sci. 1 (1993) 48.

[27] J.S. Kasper, J.S. Prener, Acta Crystallogr. 7 (1954) 246.

[28] M. Partik, M. Schneider, H.D. Lutz, Z. Anorg, Allg. Chem. 620 (1994) 791.

[29] R. Hofstadter, E.W. O'Dell, C.T. Schmidt, Rev. Sci. Instrum. 36 (1964) 246.

[30] S.S. Novosad, I.S. Novosad, Inorg. Mater. 45 (2009) 198, https://doi.org/10.1134/S0020168509020162.

[31] D.H. Gahane, N.S. Kokode, P.L. Muthal, S.M. Dhopte, S.V. Moharil, Opt. Mater. 32 (2009) 18−21.

[32] R.J. Yu, J. Wang, M. Zhang, J.H. Zhang, H.B. Yuan, Q. Su, Chem. Phys. Lett. 453 (2008) 197.

[33] S.J. Dhoble, K.N. Shinde, Adv. Mat. Lett. 2 (2011) 349.

[34] A.H. Mckeag, P.W. Ranby, British Patent No. 578 192, 1942.

[35] K.H. Butler, Fluorescent Lamp Phosphors, University Press, London, 1986.

[36] T. Welker, J. Lumin. 48 & s49 (1991) 49.

[37] J.P. Budin, J.C. Michel, F. Auzel, J. Appl. Phys. 50 (1979) 641.

[38] K. Kamiya, M. Tanahashi, T. Suzuki, K. Tanaka, Mater. Res. Bull. 25 (1990) 63.

[39] A.H. McKeag, P.W. Ranby, Ind. Chem. 513 (1947) 597.

[40] H.G. Jenkins, A.H. Mckeag, P.W. Ranby, J. Electrochem. Soc. 96 (1949) 1.

[41] R. Nagy, R.W. Wollentin, C.K. Lui, Ibid 95 (1949) 187.

[42] K.H. Butler, Llum. Eng. 44 (1949) 267.

[43] P.D. Johnson, in: P. Goldberg (Ed.), Luminescence of Inorganic Solids, Academic Press, New York, USA, 1966.

Phosphor Handbook: Process, Properties, and Applications provides a comprehensive overview of the latest advances in research on the synthesis, characterization, and applications of organic and inorganic phosphors. There is detailed information presented on the characterization of the relevant phosphor groups, such as upconversion and downconversion phosphors, inorganic LED phosphors, organic LED phosphors, and thermoluminescence and dosimetric phosphors using various physical and chemical advances. Finally, advances in phosphor technologies are discussed, including current barriers to their use in commercial applications and emerging opportunities. This book is suitable for researchers and practitioners in academia and those working in R&D in industry in the disciplines of materials science and engineering, materials chemistry, materials physics, photonics science and technology, nanotechnology, and physical chemistry.

Key Features

- Introduces fundamentals of phosphor materials, including their mechanisms, properties, and technologies
- Reviews the most important categories of phosphor materials (inorganic and organic) for use in light-emitting diodes and dosimetry
- Discusses advances in physical and chemical methods to synthesize and characterize phosphor materials

About the Editors

Vijay B. Pawade
Assistant Professor, Department of Applied Physics, Laxminarayan Institute of Technology, R.T.M. Nagpur University, Nagpur, India
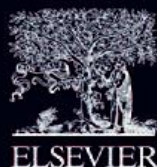
Ritesh L. Kohale
Assistant Professor and Head of Department, SGM College, Nagpur, Maharashtra, India

Sanjay J. Dhoble
Professor, Department of Physics, R.T.M. Nagpur University, Nagpur, Maharashtra, India

Hendrik C. Swart
Senior Professor, Department of Physics, University of Free State, Bloemfontein, South Africa